

ADSORPTION OF CEFIXIME TRIHYDRATE ONTO CHITOSAN 10B FROM AQUEOUS SOLUTION: KINETIC, EQUILIBRIUM AND THERMODYNAMIC STUDIES

GAZI MD. SALAH UDDIN, SOMA SAHA, SUBARNA KARMAKER and
TAPAN KUMAR SAHA

Department of Chemistry, Jahangirnagar University, Savar, Dhaka 1342, Bangladesh
✉ *Corresponding author: T. K. Saha, tksaha_ju@yahoo.com*

Received April 13, 2021

An efficient and biodegradable adsorbent chitosan 10B was used to eliminate cefixime trihydrate from aqueous solution. The kinetic behavior of cefixime trihydrate adsorption onto chitosan 10B was studied in aqueous medium, from various operational aspects, such as contact time, solution pH, antibiotic concentrations, and temperatures. Cefixime adsorption onto chitosan 10B was confirmed by Fourier transform infrared spectroscopy (FTIR), field emission scanning electron microscopy (FE-SEM) and energy-dispersive X-ray spectroscopy (EDX). The antibiotic adsorption kinetics obeyed a pseudo-second-order model rather than pseudo-first-order and Elovich kinetic models. The best illustration of antibiotic adsorption equilibrium was made by the Langmuir model, with the highest adsorption ability q_m : 37.04 $\mu\text{mol/g}$ at 298 K. The activation energy (E_a) of the present adsorption system was computed to be 44.18 kJ/mol. The values of activation (ΔG^\ddagger , ΔH^\ddagger and ΔS^\ddagger) and thermodynamic (ΔG , ΔH and ΔS) parameters confirmed that the cefixime trihydrate adsorption onto chitosan 10B in aqueous medium is an exothermic physisorption process. Cefixime desorption from antibiotic-loaded chitosan 10B was performed in 0.1 M NaOH solution and the recycled adsorbent was utilized for a second time without significant loss of its adsorption capacity.

Keywords: adsorption, kinetics, equilibrium, thermodynamics, chitosan 10B, cefixime trihydrate

INTRODUCTION

Antibiotics are critically important, life-saving medicines for human and veterinary treatment, but a part of them gets into medical and veterinary wastewater. The presence of excess antibiotics in wastewater leads to the development of antibiotic resistant microorganisms.^{1,2} Such microorganisms change their response to medicines. Humans or animals infected with antibiotic resistant microorganisms are harder to treat, compared to patients infected with non-resistant bacteria.³⁻⁵ Therefore, the removal of these antibiotics from wastewater is an urgent need to protect humans, animals and the aquatic environment.

Various treatment methods, such as adsorption,⁶⁻⁹ degradation,^{10,11} photodegradation,^{12,13} reverse osmosis,¹⁴ oxidation,¹⁵ coagulation/sedimentation,¹⁶ and ultraviolet irradiation at disinfection dosages,^{17,18} have been utilized to eliminate antibiotics from water.

Adsorption is believed to be a useful and economical technique to eliminate antibiotics from wastewater. Different types of adsorbents, such as activated carbon,^{19,20} walnut shell,²¹ bamboo charcoal,²² carbon nanotubes²³ etc., have been used to remove antibiotics from water. Activated carbon is considered to be an effective adsorbent, but it is quite expensive to produce. Thus, the utilization of low-cost, biodegradable and plentiful biosorbents is most desirable for eliminating antibiotics from wastewater. Many researchers are in search of economically feasible adsorbents, with high adsorption performance. Chitosan, modified chitosan and magnetic chitosan nanocomposites have been used as efficient adsorbents for removing dyes and metal ions from aqueous solution.²⁴⁻³² Chitosan is synthesized by treating chitin with sodium hydroxide. Chitin is a natural polysaccharide obtained from hard shells of shrimps, crabs, krill and lobsters.³³

Cefixime (Fig. 1a), a semisynthetic third-generation cephalosporin antibiotic, is commonly used to treat a wide variety of bacterial infections, such as bronchitis, gonorrhoea, infections in throats, ears, tonsils, urinary tracts *etc.* It has an expanded spectrum of bactericidal activity.³⁴ The possibility of cefixime contamination of the aquatic environment is high. If microorganisms become resistant to cefixime, this can lead to very serious consequences. It has been reported that polyelectrolyte-modified nanosilica (PMNS),³⁵ perlite-modified Portland cement,³⁶ and electro-synthesized³⁷ Mg(OH)₂ have been utilized as adsorbents to eliminate cefixime from water. However, the cefixime elimination efficiency of these adsorbents is inadequate. Therefore, an efficient adsorbent is needed to remove this antibiotic from aqueous solution.

In our review of the published literature, we found that chitosan and modified chitosan have been used to eliminate antibiotics, such as amoxicillin,³⁸ levofloxacin, ceftriaxone³⁹ and cefotaxime,⁴⁰ from aqueous solution. Therefore,

in the present study, chitosan 10B (Fig. 1b) has been chosen to eliminate cefixime trihydrate from aqueous solution. The influence of contact time, solution pH, antibiotic concentration and temperature on the kinetics of cefixime adsorption onto chitosan 10B was examined in aqueous medium. Various kinetic models and isotherm equations were utilized to explain the results found in batch adsorption kinetics and equilibrium adsorption experiments. Error analysis was also conducted in this study. The antibiotic adsorption onto chitosan 10B was confirmed by Fourier transform infrared spectroscopy (FTIR), field emission scanning electron microscopy (FE-SEM) and energy-dispersive X-ray spectroscopic (EDX) analysis. The cefixime adsorption ability of chitosan 10B was compared with that of other adsorbents described in the literature. The activation parameters and thermodynamics of the adsorption process were evaluated. The reuse of cefixime-loaded chitosan 10B was also examined.

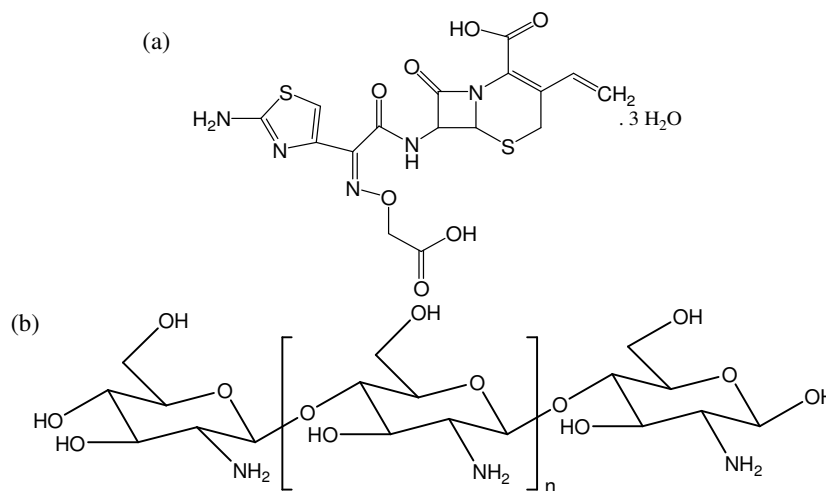


Figure 1: Structures of cefixime trihydrate (a) and chitosan 10B (b)

EXPERIMENTAL

Chemicals

Chitosan 10B (100% deacetylated chitin; Funakoshi Co. Ltd., Japan), cefixime trihydrate (Sigma-Aldrich, Germany), sodium hydroxide and hydrochloric acid (Merck, Germany) were used as received. All other chemicals used in the present study were of reagent grade and were obtained from Merck, Germany. Deionized water was produced by flowing distilled water across a deionizing column (Branstead, Syboron Corporation, Boston, USA).

Batch adsorption experiments

The batch adsorption studies were carried out in stoppered bottles with a measured quantity (0.03 g) of chitosan 10B and 25 mL of 50 $\mu\text{mol/L}$ cefixime solution.²⁴ The stock solution of cefixime was prepared by dissolving the cefixime trihydrate in deionized water. The pH of the cefixime solution was controlled with 0.1 mol/L HCl and 0.1 mol/L NaOH. The solution pH was determined by a pH meter (Adwa AD8000). The reagent bottles containing the solutions were stirred in a water bath shaking incubator at room temperature (25 ± 0.2 °C), with a continual velocity

(120 rpm) until equilibrium. The bottles containing the adsorption samples were kept closed to avoid evaporation. The samples were withdrawn at definite time intervals for determining the concentration of cefixime in solution. The samples were centrifuged at 4000 rpm for 5 min. The concentration of cefixime in the supernatant was computed by the spectrophotometric method, using a UV-1800 spectrophotometer (Shimadzu, Japan), at λ_{\max} of 289 nm (pH 3-8). The molar absorptivity of cefixime was estimated to be 22.9×10^3 L/mol.cm at 289 nm. The amount of cefixime adsorbed per gram of chitosan 10B at time t , q_t ($\mu\text{mol/g}$) was computed by using Equation (1)²⁴:

$$q_t = \frac{(C_0 - C_t) \times V}{m} \quad (1)$$

where C_0 ($\mu\text{mol/L}$) is the concentration of cefixime solution at zero time, C_t ($\mu\text{mol/L}$) is the concentration of cefixime solution at time t , V (L) is the volume of cefixime solution and m (g) is the amount of chitosan 10B used.

The antibiotic adsorption kinetics was also investigated by varying the solution pH (3-8), initial antibiotic concentrations (30, 40, 70 and 100 $\mu\text{mol/L}$) and temperatures (298, 303, 308, 313 and 318 K), respectively. The degree of antibiotic adsorption, q_t ($\mu\text{mol/g}$), was determined by a similar process as described earlier.

The equilibrium antibiotic adsorption onto chitosan 10B was studied in aqueous medium (pH 5) at five different temperatures (298, 303, 308, 313 and 318 K). The extent of cefixime adsorption onto chitosan 10B at equilibrium time, q_e ($\mu\text{mol/g}$), was estimated by using Equation (2)²⁴:

$$q_e = \frac{(C_0 - C_e) \times V}{m} \quad (2)$$

where C_e ($\mu\text{mol/L}$) is the concentration of cefixime solution at equilibrium time; C_0 ($\mu\text{mol/L}$), V (L) and m (g) have similar significance as previously mentioned.

The Fourier transform infrared (FTIR) spectra of chitosan 10B and cefixime-loaded chitosan 10B were measured in KBr by employing an FTIR spectrometer (IRPrestige-21 FTIR Spectrophotometer, Shimadzu, Japan), in the wavenumber range of 400-4000 cm^{-1} . Surface morphology and elemental analysis of chitosan 10B were studied by using field emission scanning electron microscopy (FE-SEM) and energy dispersive X-ray (EDX) analysis (JSM-7610F Schottky field emission scanning electron microscope, JEOL Ltd., Japan) before and after adsorption of cefixime.

In the desorption experiment, the eluent was 0.1 mol/L NaOH solution. At first, chitosan 10B (0.03 g) was shaken with 50 $\mu\text{mol/L}$ cefixime solution (25 mL; pH 3) for 240 min and filtered. The antibiotic-loaded chitosan 10B was dried at room temperature overnight and placed into eluent (25 mL) for the desorption experiment. The sample was agitated for 120 min. The amount of antibiotic adsorption was computed in a similar way as mentioned earlier. Regenerated chitosan

10B was cleaned thoroughly with distilled water until pH was neutral. The regenerated adsorbent was then dried at 100 °C and weighed and used again for the next adsorption experiment. All the data reported in this study were the average of double measurements.

RESULTS AND DISCUSSION

Effect of contact time

The influence of interaction time on cefixime adsorption capacity, q_t ($\mu\text{mol/g}$), of chitosan 10B in aqueous medium (pH 3) is presented in Figure 2. The antibiotic adsorption rate was rapid during the initial 90 minutes, then, it declined slowly and attained equilibrium within 180 min. At the beginning, the large surface area of the adsorbent was available for the adsorbate, which supported the initial rapid adsorption of cefixime onto chitosan 10B. When the external surface of chitosan 10B was saturated by cefixime molecules, the adsorption rate slowed down and the antibiotic molecules started to penetrate into the internal pores of the adsorbent, with a slower rate.⁴¹ After reaching equilibrium, there was no significant improvement in the extent of antibiotics adsorption over time. However, data were recorded for 240 minutes to establish an absolute equilibrium adsorption, which was kept as constant equilibrium time for the following studies.

Effect of solution pH

The adsorption behavior of cefixime onto chitosan 10B in aqueous medium is pH dependent as the charge properties of cefixime and chitosan 10B have been altered with changing solution pH. The time profiles of cefixime adsorption onto chitosan 10B in aqueous solution (pH 3-8) are depicted in Figure 3a. The initial adsorption rate and cefixime adsorption capacity of chitosan 10B, q_t ($\mu\text{mol/g}$), diminished with rising solution pH. The adsorbed quantity of cefixime at equilibrium, q_e ($\mu\text{mol/g}$), onto chitosan 10B at different solution pH is exhibited in Figure 3b. The values of q_e were found to be 40.86 $\mu\text{mol/g}$ at pH 3 and 18.93 $\mu\text{mol/g}$ at pH 8. The results may be explained with the help of pH_{zpc} of chitosan and pK_a of cefixime. We know that the solution pH affects both the binding sites of chitosan 10B and the ionic nature of cefixime. The pH_{zpc} of chitosan is reported to be 6.3.⁴² Sanil *et al.*⁴³ stated that the pK_a values of cefixime are 2.77, 3.42 and 4.17. These facts suggest that the surface of chitosan 10B became poly-cationic nature at $\text{pH} < \text{pH}_{\text{zpc}}$ of chitosan, and hence the highest degree of

cefixime elimination with chitosan 10B occurred in aqueous medium at pH 3 (Fig. 3b). The extent of antibiotic elimination with chitosan 10B decreased with a rising solution pH, because the surface of chitosan 10B developed a poly-anionic character at solution pH > pH_{zpc} of chitosan, which causes electrostatic repulsion between chitosan 10B and cefixime anions.⁴⁴ Hence, all other kinetic experiments were performed in aqueous solution at pH 3.

Effect of initial antibiotic concentration

To explore the adsorption kinetics, the extent of cefixime adsorption was investigated at four different concentrations of antibiotic (30, 40, 70 and 100 $\mu\text{mol/L}$) in aqueous solution (pH 3), with a fixed amount of chitosan 10B (0.03 g) at 298 K. The changes in cefixime adsorption, q_t ($\mu\text{mol/g}$),

onto chitosan 10B with interaction time, t (min), at various cefixime concentrations, are shown in Figure 4. It is observed that the initial rate, h ($\mu\text{mol/g min}$), and the amount of antibiotic adsorption onto chitosan 10B, q_e ($\mu\text{mol/g}$), were intensified with rising cefixime concentration (Table 1). With rising antibiotic concentration from 30 to 100 $\mu\text{mol/L}$, the values of q_e increased from 24.23 to 77.81 $\mu\text{mol/g}$ (Fig. 4). The results suggest that the initial concentration of antibiotic in solution gives essential driving forces to overwhelm all mass transfer resistances between the adsorbate and the adsorbent, favoring adsorption.²⁴ Similar results were also noticed in the elimination of reactive blue 4 (RB4) and reactive black 5 (RB5) by chitosan from aqueous solution.^{44,45}

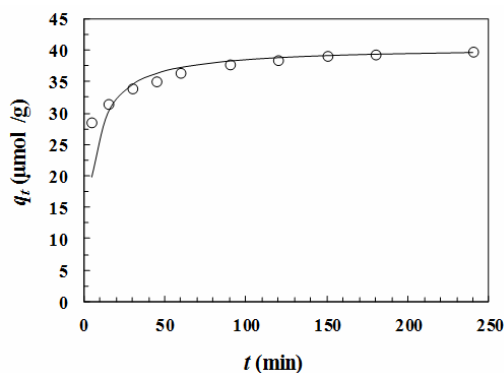


Figure 2: Plot of q_t versus t for cefixime adsorption onto chitosan 10B in aqueous medium at 298 K ([cefixime]₀: 50 $\mu\text{mol/L}$; pH: 3; volume of antibiotic solution: 25 mL; amount of chitosan 10B: 0.03 g). Solid line exhibits the pseudo-second-order adsorption kinetic trace developed by using Equation (4) and values of $q_{e(\text{cal})}$ and k_2 recorded in Table 1

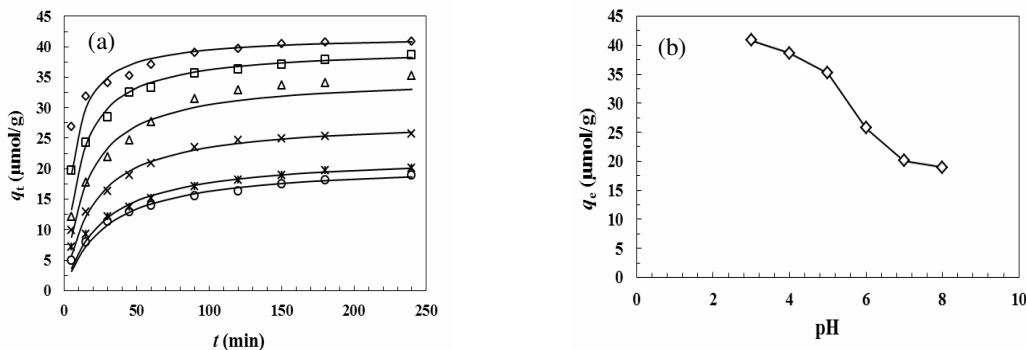


Figure 3: (a) Influence of solution pH on cefixime adsorption onto chitosan 10B from aqueous medium at 298 K ([cefixime]₀: 50 $\mu\text{mol/L}$; volume of antibiotic solution: 25 mL; amount of chitosan 10B: 0.03 g; solution pH: \diamond pH 3; \square pH 4; Δ pH 5; \times pH 6; $*$ pH 7; \circ pH 8). All lines exhibit pseudo-second-order adsorption kinetic traces formed by using Equation (4) and values of $q_{e(\text{cal})}$ and k_2 from Table 1; (b) Plot of q_e versus solution pH for cefixime adsorption onto chitosan 10B in aqueous medium at 298 K (necessary data obtained from Fig. 3a)

Table 1
Comparison of $q_{e(cal.)}$ and $q_{e(exp.)}$ values, and kinetic parameters of various kinetic models

Parameter	$q_{e(exp.)}$ ($\mu\text{mol/g}$)	Pseudo first-order model			Pseudo second-order model				Elovich kinetic model		
		$q_{e(cal.)}$ ($\mu\text{mol/g}$)	k_1 (min^{-1})	R^2	$q_{e(cal.)}$ ($\mu\text{mol/g}$)	k_2 ($\text{g}/\mu\text{mol}\cdot\text{min}$)	h (g/min)	R^2	α ($\mu\text{mol/g}$ min)	β ($\text{g}/\mu\text{mol}$)	R^2
pH: [Cefixime] ₀ : 50 $\mu\text{mol/L}$; Temperature 298 K; adsorbent dosage: 0.03 g											
3	40.86	15.71	24.87×10^{-3}	0.989	41.84	4.03×10^{-3}	7.06	0.999	1.06×10^3	0.265	0.986
4	38.62	16.82	17.27×10^{-3}	0.979	39.84	2.52×10^{-3}	3.99	0.999	4.65×10^1	0.193	0.981
5	35.21	22.48	17.73×10^{-3}	0.988	35.09	1.90×10^{-3}	2.34	0.998	7.58×10^1	0.153	0.986
6	25.75	17.54	21.65×10^{-3}	0.997	28.09	1.82×10^{-3}	1.44	0.999	6.49×10^1	0.217	0.976
7	20.07	14.85	18.65×10^{-3}	0.982	22.22	1.76×10^{-3}	0.87	0.999	3.93×10^1	0.273	0.983
8	18.93	13.34	15.20×10^{-3}	0.983	20.83	1.72×10^{-3}	0.75	0.998	5.57×10^1	0.267	0.996
[Cefixime] ₀ ($\mu\text{mol/L}$); pH 3; Temperature 298 K; adsorbent dosage: 0.03 g											
100	77.81	7.38	23.72×10^{-3}	0.982	77.52	10.27×10^{-3}	61.73	1.000	3.25×10^{14}	0.489	0.972
70	52.56	5.55	18.89×10^{-3}	0.967	53.19	11.01×10^{-3}	31.15	1.000	3.64×10^{10}	0.545	0.968
40	31.35	5.24	32.24×10^{-3}	0.921	31.75	14.68×10^{-3}	14.79	0.999	6.44×10^5	0.555	0.911
30	24.23	2.03	14.74×10^{-3}	0.934	24.27	26.61×10^{-3}	15.67	1.000	1.47×10^{12}	1.386	0.960
Temperature (K); [Cefixime] ₀ : 50 $\mu\text{mol/L}$; pH 3; adsorbent dosage: 0.03 g											
298	39.76	11.03	18.89×10^{-3}	0.995	40.49	4.73×10^{-3}	7.75	0.999	6.52×10^3	0.326	0.992
303	37.94	10.40	21.65×10^{-3}	0.996	38.61	5.72×10^{-3}	8.53	0.999	1.25×10^3	0.254	0.985
308	36.08	9.04	21.88×10^{-3}	0.982	36.63	6.73×10^{-3}	9.03	0.999	4.68×10^3	0.346	0.959
313	33.55	6.05	19.12×10^{-3}	0.923	33.90	9.46×10^{-3}	10.87	0.999	3.51×10^4	0.439	0.944
318	29.65	3.38	13.13×10^{-3}	0.829	29.76	15.03×10^{-3}	13.32	0.999	4.39×10^6	0.677	0.910

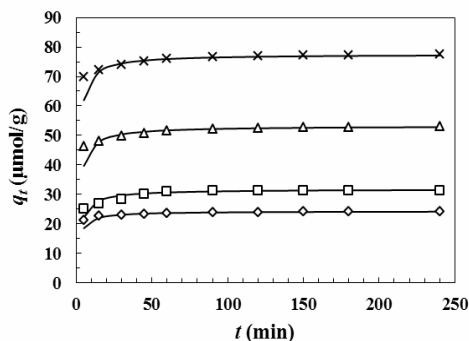


Figure 4: Plots of q_t versus t for cefixime adsorption onto chitosan 10B from aqueous medium at various initial antibiotic concentrations and at 298 K. (Volume of antibiotic solution: 25 mL; pH: 3; amount of chitosan 10B: 0.03 g; [Cefixime]₀: \diamond 30 $\mu\text{mol/L}$; \square 40 $\mu\text{mol/L}$; Δ 70 $\mu\text{mol/L}$; \times 100 $\mu\text{mol/L}$). All lines exhibit pseudo-second-order adsorption kinetic traces formed by using Equation (4) and values of $q_{e(\text{cal})}$ and k_2 from Table 1

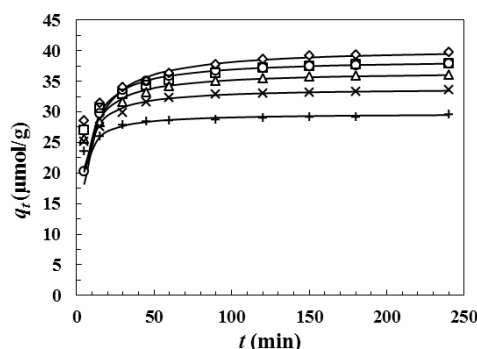


Figure 5: Effects of temperature on cefixime adsorption onto chitosan 10B in aqueous medium. ([cefexime]₀: 50 $\mu\text{mol/L}$; pH: 3; volume of antibiotic solution: 25 mL; amount of chitosan 10B: 0.03 g; solution temperatures: \diamond 298 K; \square 303 K; Δ 308 K; \times 313 K; + 318 K). All lines exhibit pseudo-second-order adsorption kinetic traces formed by using Equation (4) and values of $q_{e(\text{cal})}$ and k_2 from Table 1

Effect of temperature

Temperature may decrease or increase the extent of adsorption, depending on whether the adsorption process is exothermic or endothermic. Cefixime adsorption kinetics was studied in aqueous medium (pH 3) at various temperatures, with a fixed concentration (50 $\mu\text{mol/L}$) of antibiotic and chitosan 10B (0.03 g) for 240 min. The results are given in Figure 5. It is noticed that the initial antibiotic adsorption rate, (h , $\mu\text{mol/g min}$), onto chitosan 10B was intensified with rising solution temperatures. However, the extent of cefixime adsorption onto chitosan 10B decreased with rising solution temperatures. The values of q_e were found to be 39.76 $\mu\text{mol/g}$ at 298 K and 29.65 $\mu\text{mol/g}$ at 318 K, respectively, indicating an exothermic adsorption process, as observed in the elimination of tetracycline from aqueous solution by tannin based cryogels (TAB CRGs).⁴⁶

Modeling of adsorption kinetics

To know the cefixime elimination kinetics, the pseudo-first-order,⁴⁷ pseudo-second-order⁴⁸ and Elovich kinetic models⁴⁹ were employed to analyze the kinetic data derived from batch experiments. The pseudo-first-order kinetic model is stated by Equation (3):⁴⁷

$$\log(q_e - q_t) = \log q_e - \frac{k_1 t}{2.303} \quad (3)$$

where q_e ($\mu\text{mol/g}$) and q_t ($\mu\text{mol/g}$) symbolize the quantity of antibiotic adsorption onto chitosan 10B at equilibrium time and at time t ,

respectively, and k_1 (min^{-1}) symbolizes the pseudo-first-order rate constant.

The pseudo-second-order kinetic model is presented by Equations (4) and (5):⁴⁸

$$\text{Non-linear form: } q_t = \frac{k_2 q_e^2 t}{(1 + k_2 q_e t)} \quad (4)$$

$$\text{Linear form: } \frac{t}{q_t} = \frac{1}{k_2 q_e^2} + \frac{1}{q_e} t \quad (5)$$

where k_2 ($\text{g}/\mu\text{mole min}$) symbolizes the pseudo-second-order adsorption rate constant. If pseudo-second-order kinetics is valid, the plot of $\left(\frac{t}{q_t}\right)$ against t should give a linear relationship.

The initial adsorption rate, h ($\mu\text{mol/g min}$), is defined by Equation (6):⁴⁸

$$h = k_2 q_e^2 \quad (6)$$

The Elovich model is usually stated by Equation (7):⁴⁹

$$q_t = \frac{1}{\beta} \ln(\alpha\beta) + \frac{1}{\beta} \ln t \quad (7)$$

where α ($\mu\text{mol/g min}$) symbolizes an initial antibiotic adsorption rate and β ($\text{g}/\mu\text{mol}$) is related to the level of surface exposure and the activation energy of chemisorption. The constants can be calculated from the plot of q_t against $\ln t$.

Table 1 presents the values of correlation coefficients (R^2) and kinetic parameters of different kinetic models. It is found that the R^2 values derived from the pseudo-first-order model (≤ 0.997) and the Elovich model (≤ 0.996) were lower compared to the R^2 values derived from the pseudo-second-order kinetic model (≥ 0.999). The observed adsorption kinetic traces (Figs. 2, 3a, 4

and 5) are fairly replicated in the mimicked data (each solid line in Figs. 2, 3a, 4 and 5) derived from the pseudo-second-order kinetic model Equation (4), using the values of k_2 and $q_{e(\text{cal.})}$ (Table 1). Additionally, the computed $q_{e(\text{cal.})}$ values derived from the pseudo-second-order kinetic model were analogous to the experimental $q_{e(\text{exp.})}$ values (Table 1). Therefore, the kinetics of cefixime elimination with chitosan 10B from aqueous medium follows the pseudo-second-order kinetic model, as found earlier for the removal of azo dyes, such as remazol brilliant violet, reactive yellow 145, RB4 and RB5, with chitosan from water.^{24,25,44,45}

Activation parameters

The activation energy (E_a) for cefixime elimination with chitosan 10B from aqueous medium was determined by Equation (8):⁵⁰

$$\ln k_2 = -\frac{E_a}{RT} + \text{constant} \quad (8)$$

where R (8.314 J/mol K) is the universal gas constant, T (K) symbolizes the solution temperature and k_2 (g/ $\mu\text{mole min}$) is the pseudo-second-order rate constant listed in Table 1. From the slope of $\ln k_2$ against $1/T$ plot ($R^2 = 0.973$), E_a was computed to be 44.18 kJ/mol in the temperature range 298-318 K. It is well known that the magnitude of E_a indicates whether the adsorption is physical ($E_a = 5 - 40$ kJ/mol) or chemical ($E_a = 40 - 800$ kJ/mol).⁵¹ The value of E_a (44.18 kJ/mol) reveals that the elimination of cefixime with chitosan 10B involves some physical adsorption.

Additionally, the changes in the enthalpy of activation (ΔH^\ddagger), entropy of activation (ΔS^\ddagger) and Gibbs free energy of activation (ΔG^\ddagger) are stated by the following equations:⁴¹

$$\ln\left(\frac{k_2}{T}\right) = -\frac{\Delta H^\ddagger}{RT} + \ln\frac{k_B}{h_P} + \frac{\Delta S^\ddagger}{R} \quad (9)$$

$$\Delta G^\ddagger = \Delta H^\ddagger - T\Delta S^\ddagger \quad (10)$$

where k_2 , R and T have similar significance as described before, k_B (1.381×10^{-23} J/K) and h_P (6.626×10^{-34} Js) symbolize the Boltzman constant and the Plank constant, respectively. From the slope and y-intercept of $\ln(k_2/T)$ versus $1/T$ ($R^2 = 0.937$) plot, ΔH^\ddagger (41.62 kJ/mol) and ΔS^\ddagger (-35.63 J/mol.K) values were estimated. The observed E_a and ΔH^\ddagger values for cefixime adsorption onto chitosan 10B agreed well with the value calculated from the activated complex theory of reaction in solution, $E_a = \Delta H^\ddagger + RT$. The $T_{\text{av}}\Delta S^\ddagger$ value was computed to be -10.97 kJ/mol,

where T_{av} symbolizes the mean value of five working temperatures in the adsorption experiments. Here, $\Delta H^\ddagger > T_{\text{av}}\Delta S^\ddagger$ suggests that the influence of enthalpy is more important than that of entropy in activation. The ΔG^\ddagger values were calculated to be 52.24, 52.42, 52.60, 52.78 and 52.96 kJ/mol at 298, 303, 308, 313 and 318 K, respectively, indicating the presence of an energy barrier in the adsorption process.⁵²

Adsorption isotherms

The investigation of adsorption isotherm data is essential to understand the relation between the adsorbate and the adsorbent used. Figure 6 represents the plots of q_e against C_e at various temperatures. It is noted that the q_e values decreased with increasing solution temperatures from 298 K to 318 K, which implies that the cefixime adsorption onto chitosan 10B is an exothermic phenomenon.

The equilibrium adsorption isotherms were interpreted by the following isotherm models: Freundlich,⁵³ Temkin⁵⁴ and Langmuir.⁵⁵ Non-linear and linear forms of these models are exhibited as:

Freundlich isotherm model:

$$\text{Non-linear form: } q_e = K_F C_e^{\frac{1}{n}} \quad (11)$$

$$\text{Linear form: } \ln q_e = \frac{1}{n} \ln C_e + \ln K_F \quad (12)$$

where q_e ($\mu\text{mol/g}$) and C_e ($\mu\text{mol/L}$) have similar significance as previously mentioned, K_F ($(\mu\text{mol/g})(\mu\text{mol/L})^{-1/n}$) and n are called Freundlich isotherm constants, indicating the ability and strength of the adsorption, respectively.

Temkin isotherm model:

$$\text{Non-linear form: } q_e = \frac{RT}{b} \ln(K_T C_e) \quad (13)$$

$$\text{Linear form: } q_e = \frac{RT}{b} \ln K_T + \frac{RT}{b} \ln C_e \quad (14)$$

where K_T ($\mu\text{mol/L}$) is the Temkin isotherm constant, b (J/mol) is a constant associated to the heat of adsorption. R (8.314 J/mol K) and T (K) have similar significance as discussed earlier.

Langmuir isotherm model:

$$\text{Non-linear form: } q_e = \frac{K_L C_e}{(1 + a_L C_e)} \quad (15)$$

$$\text{Linear form: } \frac{C_e}{q_e} = \frac{1}{K_L} + \frac{a_L}{K_L} C_e \quad (16)$$

where K_L (L/g) and a_L (L/ μmol) are the characteristic constants of the Langmuir equation, and the K_L/a_L ratio provides the highest antibiotic adsorption capacity, q_m ($\mu\text{mol/g}$), of chitosan

10B. Table 2 presents the values of isotherm parameters and correlation coefficients (R^2). In every case, the Langmuir isotherm model has the highest values of correlation coefficients (R^2), compared to the Freundlich and Temkin isotherms. The experimental adsorption isotherms (Fig. 6) are completely replicated in the mimicked isotherms (each solid line in Fig. 6) derived from the Langmuir isotherm model Equation (15), using the values of K_L and a_L recorded in Table 2. Hence, all the adsorption isotherms are explained well by the Langmuir model, and the highest cefixime adsorption ability of chitosan 10B was computed to be 37.04 $\mu\text{mol/g}$ at 298 K. The highest values of correlation coefficient (R^2) from the Langmuir isotherm suggest monolayer coverage of cefixime antibiotic on chitosan 10B surface.

The separation factor, R_L (Table 3), was employed to describe the features of the Langmuir isotherm. R_L is stated by Equation (17):⁵⁶

$$R_L = \frac{1}{(1+a_L C_0)} \quad (17)$$

where a_L ($\text{L}/\mu\text{mol}$) is the Langmuir isotherm constant and C_0 ($\mu\text{mol/L}$) symbolizes the maximum initial concentration of antibiotic employed in the isotherm studies. The values of R_L were estimated to be 0.048, 0.061, 0.091, 0.087 and 0.123 for chitosan 10B at 298, 303, 308, 313 and 318 K, respectively, indicating favorable adsorption at all the mentioned temperatures.⁴² Five different error functions, such as the sum of the squares of errors (SSE), the sum of the absolute errors (SAE), the average relative error (ARE), the hybrid fractional error function (HYBRID) and Marquardt's percent standard deviation (MPSD), were considered to obtain the best fitting isotherm model for the present adsorption process.⁵⁷

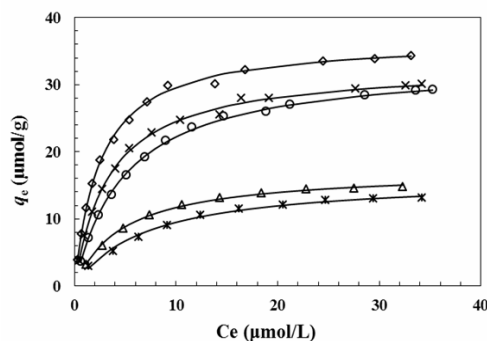


Figure 6: Adsorption isotherm of cefixime onto chitosan 10B at various temperatures ($[\text{Cefixime}]_0$: 5-70 $\mu\text{mol/L}$; pH: 5; volume of antibiotic solution: 25 mL; amount of chitosan 10B: 0.03 g; Temperatures: \diamond 298 K; \times 303 K; \circ 308 K; \triangle 313 K; $+$ 318 K). All solid lines are obtained from Langmuir model using Equation (15) and K_L and a_L values recorded in Table 2

Table 2

Various isotherm parameters obtained for cefixime adsorption onto chitosan 10B in aqueous solution (pH 5) at different temperatures

Isotherms	Parameters	Temperatures (K)				
		298	303	308	313	318
Langmuir model	K_L (L/g)	14.71	9.62	6.67	3.64	2.30
	a_L ($\text{L}/\mu\text{mol}$)	0.40	0.31	0.20	0.21	0.14
	q_m ($\mu\text{mol/g}$)	37.04	31.03	33.34	17.23	16.11
	R^2	0.998	0.999	0.998	0.999	0.997
Freundlich model	K_F ($(\mu\text{mol/g})(\mu\text{mol/L})^{-1/n}$)	9.55	7.42	5.93	3.75	2.84
	n	1.86	1.90	1.76	2.27	2.11
	R^2	0.943	0.950	0.970	0.934	0.965
Temkin model	K_T ($\mu\text{mol/L}$)	4.48	3.31	2.25	2.18	1.46
	b_T (J/mol)	323.90	366.84	353.15	678.94	710.70
	R^2	0.990	0.992	0.985	0.986	0.984

Table 3
Significance of R_L values

Values of R_L	$R_L > 1.0$	$0 > R_L < 1.0$	$R_L = 1.0$	$R_L = 0$
Types of adsorption	Unfavorable	Favorable	Linear	Irreversible

Table 4
Isotherm error analysis for cefixime adsorption onto chitosan 10B

Isotherms	SSE	SAE	ARE	HYBRID	MPSD
Temperature: 298 K					
Langmuir	2.54	3.69	2.06	3.44	3.46
Freundlich	104.19	21.32	12.27	20.46	21.01
Temkin	8.12	7.63	6.72	11.19	13.97
Temperature: 303 K					
Langmuir	2.03	3.38	1.98	3.30	3.13
Freundlich	57.05	19.72	12.19	20.31	18.36
Temkin	4.80	6.53	5.93	9.89	11.77
Temperature: 308 K					
Langmuir	0.93	2.70	1.81	3.02	2.68
Freundlich	40.52	14.34	8.94	14.90	14.14
Temkin	8.05	7.77	8.87	14.78	20.08
Temperature: 313 K					
Langmuir	0.35	1.66	1.81	3.02	2.95
Freundlich	16.83	10.87	10.58	17.63	16.08
Temkin	2.02	3.81	3.63	6.05	5.63
Temperature: 318 K					
Langmuir	0.68	2.18	3.29	5.49	6.04
Freundlich	8.60	7.36	7.60	12.67	11.36
Temkin	1.82	3.72	5.44	9.06	9.80

Error analysis was employed for the Langmuir, Freundlich and Temkin adsorption isotherms (Table 4). From the error analysis data, it has been also noticed that the Langmuir adsorption isotherm model was the best fitting model for cefixime adsorption onto chitosan 10B in aqueous medium.

Table 5 illustrates the comparison of cefixime adsorption capacity (q_{\max} , $\mu\text{mol/g}$) of chitosan 10B with that of other adsorbents reported in the literature. The q_{\max} ($\mu\text{mol/g}$) value of chitosan 10B in the current study confirmed that it is an efficient adsorbent to eliminate cefixime from aqueous media.

Confirmation of cefixime adsorption onto chitosan 10B by FTIR, SEM and EDX

The FTIR spectra of chitosan 10B taken in KBr before and after cefixime adsorption are shown in Figure 7. The broad band at 3444 cm^{-1}

associated with N-H and O-H stretching of chitosan 10B (Fig. 7a) shifted to 3450 cm^{-1} in cefixime-loaded chitosan 10B (Fig. 7b), which is ascribed to the interaction between the OH/NH group of chitosan 10B and antibiotic molecules.⁵⁸ The band at 2920 cm^{-1} corresponding to C-H stretching in the spectra of fresh chitosan 10B shifted to 2924 cm^{-1} after adsorption. The vibration bands at 1635 cm^{-1} for amide-I (C=O stretching) and at 1560 cm^{-1} for amide-II (N-H bending) of fresh chitosan 10B (Fig. 7a) shifted to 1597 cm^{-1} in cefixime-loaded chitosan 10B (Fig. 7b). The peaks appearing at 1427 cm^{-1} for $-\text{CH}_2$ bending, at 1385 cm^{-1} for C-H bending, at 1153 cm^{-1} for coinciding C-O-C and C-O stretching, and at 1077 cm^{-1} for C-O stretching of fresh chitosan 10B (Fig. 7a) shifted to 1421 cm^{-1} , 1384 cm^{-1} , 1152 cm^{-1} and 1093 cm^{-1} , as depicted in Figure 7b. Hence, the adsorption of cefixime onto chitosan 10B can be confirmed.

Table 5
Comparison of cefixime adsorption abilities (q_{max}) of various adsorbents

Adsorbents	pH	Temperature (K)	q_{max} ($\mu\text{mol/g}$)	References
Polyelectrolyte-modified nanosilica (PMNS)	4.0	298	20.49	35
Perlite modified Portland cement	6.7	298	13.77	36
Electrosynthesized $\text{Mg}(\text{OH})_2$	7.0	303	25.40	37
Chitosan 10B	5.0	298	37.04	This study

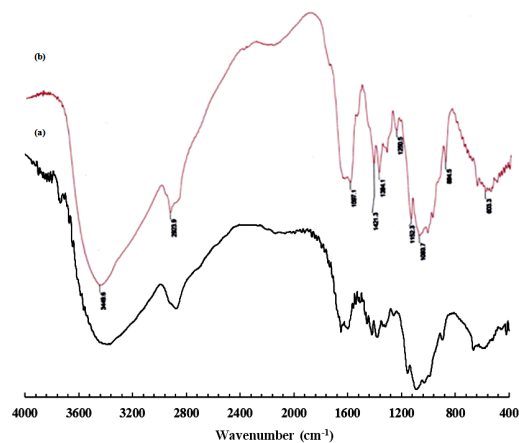


Figure 7: FTIR spectra of chitosan 10B (a) and cefixime-loaded chitosan 10B (b) (recorded in KBr)

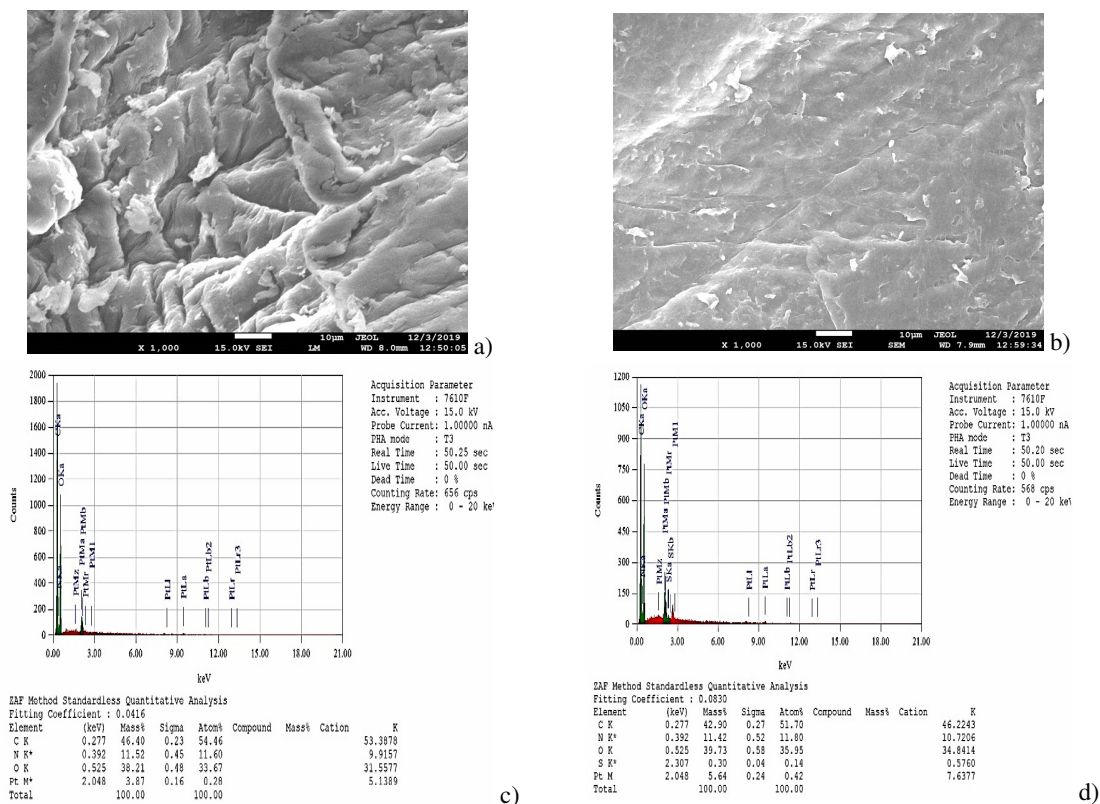


Figure 8: FE-SEM images and EDX data of chitosan 10B before (a and c) and after (b and d) adsorption of cefixime

The morphological properties of chitosan 10B were studied by field emission scanning electron microscopy (FE-SEM), along with energy dispersive X-ray (EDX) spectroscopy, before and after cefixime adsorption. The FE-SEM images and EDX data of chitosan 10B and cefixime-loaded chitosan 10B are shown in Figure 8. The surface of chitosan 10B was heterogeneous, irregular and porous before adsorption of cefixime (Fig. 8a). A comparatively smooth and homogeneous surface was detected in the FE-SEM image of cefixime-loaded chitosan 10B (Fig. 8b). This phenomenon occurred due to the filling of the surface pores of chitosan 10B by cefixime molecules, thus, the entire external surface of chitosan 10B was covered by a thin layer of cefixime. Moreover, the atom percentage of nitrogen and oxygen increased and sulphur was detected in the EDX data of cefixime-loaded chitosan surface (Fig. 8c & d). Hence, it is proven that the cefixime adsorption took place on the surface of chitosan 10B.⁵⁹

Thermodynamics

Thermodynamic parameters, *i.e.*, changes in Gibb's free (ΔG), enthalpy (ΔH), and entropy (ΔS), were estimated by using the Langmuir isotherm constant (a_L) and the following equations:⁶⁰

$$\Delta G = -RT \ln a_L \quad (18)$$

$$\ln a_L = \frac{\Delta S}{R} - \frac{\Delta H}{RT} \quad (19)$$

where R (8.314 J/mol K) and T (K) have similar significance as previously mentioned. The slope and y -intercept of $\ln a_L$ against $1/T$ plot ($R^2 = 0.929$) were utilized to determine ΔH and ΔS . The values of thermodynamic parameters are listed in Table 6. The negative ΔG and ΔH values imply that the cefixime adsorption onto chitosan 10B is a spontaneous exothermic process in nature. The negative ΔS value reveals that the adsorbed cefixime molecules on chitosan 10B surface were well organized, compared to the situation in aqueous phase.⁶¹

Table 6
Thermodynamics of cefixime adsorption onto chitosan 10B in aqueous media

Temperatures (K)	Thermodynamic parameters			R^2
	ΔG (kJ/mol)	ΔH (kJ/mol)	ΔS (J/mol.K)	
298	-31.80			
303	-31.69			
308	-31.58	-38.35	-21.70	0.929
313	-31.47			
318	-31.36			

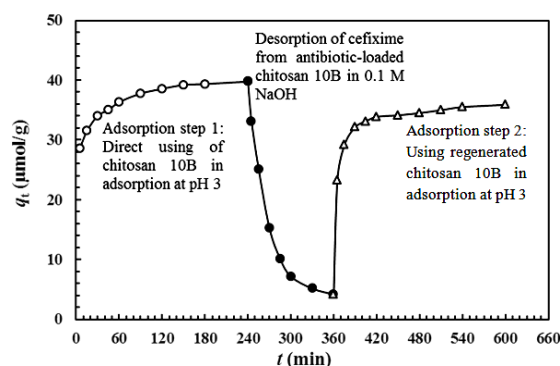


Figure 9: Adsorption–desorption–adsorption phenomena of cefixime onto chitosan 10B in aqueous solution at 298 K. ($[cefixime]_0$: 50 $\mu\text{mol/L}$; volume of antibiotic solution: 25 mL; amount of chitosan 10B: 0.03 g; \circ : adsorption step 1, pH 3; \bullet : desorption step, pH 13; Δ : adsorption step 2, pH 3 and regenerated chitosan 10B was used)

Reuse of chitosan 10B

Figure 9 shows the typical cefixime adsorption–desorption–adsorption onto chitosan

10B. In the adsorption step 1, chitosan 10B (0.03 g) was added to the 50 $\mu\text{mol/L}$ cefixime solution (25 mL) and agitated for 240 min at 298 K, while

the discharge of antibiotic from cefixime-loaded chitosan 10B was measured in 0.1 mol/L NaOH for 120 min at 298 K. The value of q_e was measured to be 40.86 $\mu\text{mol/g}$ in the adsorption step 1. In the desorption step, the cefixime release rate was quick during the initial 30 min and 95% of the antibiotic was discharged from cefixime-loaded chitosan 10B in 120 min. It suggests that the electrostatic interaction between cefixime molecules and chitosan 10B was much weaker in a basic solution. In the adsorption step 2, recycled chitosan 10B was used to adsorb 50 $\mu\text{mol/L}$ cefixime solution (pH 3) for 240 min. A similar cefixime adsorption pattern was noticed as noticed in the first adsorption step. The value of q_e was found to be 38.62 $\mu\text{mol/g}$ for recycled chitosan 10B. This result indicates that the chitosan 10B can be utilized as an eco-friendly adsorbent for eliminating cefixime from aqueous solution effectively.

CONCLUSION

A successful application of adsorption requires the development of cheap adsorbents from abundant raw materials, with identified kinetic parameters and adsorption behavior. The kinetics and equilibrium adsorption of cefixime onto chitosan 10B were examined in aqueous solution. The time required for reaching equilibrium adsorption was estimated to be 240 min. The cefixime adsorption rate onto chitosan 10B was significantly influenced by solution pH and initial antibiotic concentrations. It has been found that the cefixime adsorption capacities of chitosan 10B decreased with increasing temperatures. Batch adsorption kinetics data obeyed by the pseudo-second-order kinetic model rather than the pseudo-first-order and Elovich kinetic models. The experimentally observed $q_{e(\text{exp.})}$ values in every case were analogous to the $q_{e(\text{cal})}$ values obtained from the pseudo-second-order kinetic model. The correlation coefficient (R^2) and the data of error analysis proved that the Langmuir model was the best fitting model for the cefixime adsorption process. The maximum cefixime adsorption ability of chitosan 10B was found to be 37.04 $\mu\text{mol/g}$ at pH 5 and 298 K. FTIR, FE-SEM and EDX data confirmed the adsorption of cefixime onto chitosan 10B. All the data of activation and thermodynamic parameters demonstrated that the cefixime adsorption onto chitosan 10B is a favorable spontaneous exothermic process. The cefixime-loaded chitosan 10B released cefixime in 0.1 mol/L NaOH

solution and the recycled chitosan 10B was reused in antibiotic adsorption. Hence, chitosan 10B could be used as an ecofriendly adsorbent to eliminate cefixime from aqueous solution.

ACKNOWLEDGEMENTS: We are thankful to the Jahangirnagar University for the research grant (FY 2020-2021) awarded to Prof. Dr. Tapan Kumar Saha to complete the present work.

REFERENCES

- ¹ R. Gothwal and T. Shashidhar, *Clean – Soil, Air, Water*, **43**, 479 (2015), <https://doi.org/10.1002/clen.201300989>
- ² S. B. Levy, *Clin. Infect. Dis.*, **33**, S124 (2001), <https://doi.org/10.1086/321837>
- ³ B. Bengtsson and C. Greko, *Ups. J. Med. Sci.*, **119**, 96 (2014), <https://doi.org/10.3109/03009734.2014.901445>
- ⁴ L. B. Rice, *Curr. Opin. Microbiol.*, **12**, 476 (2009), <https://doi.org/10.1016/j.mib.2009.08.001>
- ⁵ J. L. Martínez, *Science*, **321**, 365 (2008), <https://doi.org/10.1126/science.1159483>
- ⁶ H. Yao, J. Lu, J. Wu, Z. Lu, P. C. Wilson *et al.*, *Water Air Soil Pollut.*, **224**, 1370 (2013), <https://doi.org/10.1007/s11270-012-1370-7>
- ⁷ N. Dorival-García, A. Zafra-Gómez, A. Navalón, J. González and J. L. Vilchez, *Sci. Total Environ.*, **442**, 317 (2013), <https://doi.org/10.1016/j.scitotenv.2012.10.026>
- ⁸ K. Yaghmaeian, G. Moussavi and A. Alahabadi, *Chem. Eng. J.*, **236**, 538 (2014), <https://doi.org/10.1016/j.cej.2013.08.118>
- ⁹ H. R. Pouretedal and N. Sadegh, *J. Water Process. Eng.*, **1**, 64 (2014), <https://doi.org/10.1016/j.jwpe.2014.03.006>
- ¹⁰ V. Homem and L. Santos, *J. Environ. Manage.*, **92**, 2304 (2011), <https://doi.org/10.1016/j.jenvman.2011.05.023>
- ¹¹ Y. Kitazono, I. Ihara, G. Yoshida, K. Toyoda and K. Umetsu, *J. Hazard. Mater.*, **243**, 112 (2012), <https://doi.org/10.1016/j.jhazmat.2012.10.009>
- ¹² S. R. Batchu, V. R. Panditi, K. E. O'Shea and P. R. Gardinali, *Sci. Total Environ.*, **470-471**, 299 (2014), <https://doi.org/10.1016/j.scitotenv.2013.09.057>
- ¹³ G. Prados-Joya, M. Sánchez-Polo, J. Rivera-Utrilla and M. Ferro-García, *Water Res.*, **45**, 393 (2011), <https://doi.org/10.1016/j.watres.2010.08.015>
- ¹⁴ M. Gholami, R. Mirzaei, R. R. Kalantary, A. Sabzali and F. Gatei, *Iran. J. Environ. Health Sci. Eng.*, **9**, 19 (2012), <https://doi.org/10.1186/1735-2746-9-19>
- ¹⁵ S. D. Jojoa-Sierra, J. Silva-Agredo, E. Herrera-Calderon and R. A. Torres-Palma, *Sci. Total Environ.*, **575**, 1228 (2017), <https://doi.org/10.1016/j.scitotenv.2016.09.201>

- ¹⁶ Z. P. Xing and D. Z. Sun, *J. Hazard. Mater.*, **168**, 1264 (2009), <https://doi.org/10.1016/j.jhazmat.2009.03.008>
- ¹⁷ C. W. McKinney and A. Pruden, *Environ. Sci. Technol.*, **46**, 13393 (2012), <https://doi.org/10.1021/es303652q>
- ¹⁸ M. T. Guo, Q. B. Yuan and J. Yang, *Water Res.*, **47**, 6388 (2013), <https://doi.org/10.1016/j.watres.2013.08.012>
- ¹⁹ J. Rivera-Utrilla, G. Prados-Joya, M. Sánchez-Polo, M. A. Ferro-García and I. Bautista-Toledo, *J. Hazard. Mater.*, **170**, 298 (2009), <https://doi.org/10.1016/j.jhazmat.2009.04.096>
- ²⁰ L. Ji, W. Chen, L. Duan and D. Zhu, *Environ. Sci. Technol.*, **43**, 2322 (2009), <https://doi.org/10.1021/es803268b>
- ²¹ G. Nazari, H. Abolghasemi and M. Esmaili, *J. Taiwan Inst. Chem. Eng.*, **58**, 357 (2016), <https://doi.org/10.1016/j.jtice.2015.06.006>
- ²² P. Liao, Z. Zhan, J. Dai, X. Wu, W. Zhang *et al.*, *Chem. Eng. J.*, **228**, 496 (2013), <https://doi.org/10.1016/j.cej.2013.04.118>
- ²³ W. Xiong, G. Zeng, Z. Yang, Y. Zhou, C. Zhang *et al.*, *Sci. Total Environ.*, **627**, 235 (2018), <https://doi.org/10.1016/j.scitotenv.2018.01.249>
- ²⁴ S. Karmaker, A. J. Nag and T. K. Saha, *Cellulose Chem. Technol.*, **53**, 373 (2019), <https://doi.org/10.35812/CelluloseChemTechnol.2019.53.38>
- ²⁵ S. Karmaker, T. Sen and T. K. Saha, *Polym. Bull.*, **72**, 1879 (2015), <https://doi.org/10.1007/s00289-015-1378-4>
- ²⁶ D. S. Franco, J. Vieillard, N. P. G. Salau and G. L. Dotto, *J. Mol. Liq.*, **304**, 112758 (2020), <https://doi.org/10.1016/j.molliq.2020.112758>
- ²⁷ M. E. González-López, A. A. Pérez-Fonseca, M. Arellano, C. Gómez and J. R. Robledo-Ortíz, *Environ. Technol. Innov.*, **19**, 100824 (2020), <https://doi.org/10.1016/j.eti.2020.100824>
- ²⁸ M. Usman, A. Ahmed, B. Yu, S. Wang, Y. Shen *et al.*, *Carbohydr. Polym.*, **255**, 11786 (2021), <https://doi.org/10.1016/j.carbpol.2020.117486>
- ²⁹ M. Frye, S. E. Vasisht, A. Atassi, D. Mazyck and J. C. Nino, *Cellulose Chem. Technol.*, **55**, 87 (2021), <https://doi.org/10.35812/CelluloseChemTechnol.2021.55.09>
- ³⁰ Y. Huang, C. Hu, Y. An, Z. Xiong, X. Hu *et al.*, *J. Hazard. Mater.*, **405**, 124195 (2021), <https://doi.org/10.1016/j.jhazmat.2020.124195>
- ³¹ S. Fan, J. Chen, C. Fan, G. Chen, S. Liu *et al.*, *J. Hazard. Mater.*, **416**, 126225 (2021), <https://doi.org/10.1016/j.jhazmat.2021.126225>
- ³² M. J. Sharifi, A. Nouralishahi, A. Hallajisani and M. Askari, *Cellulose Chem. Technol.*, **55**, 185 (2021), <https://doi.org/10.35812/CelluloseChemTechnol.2021.55.20>
- ³³ M. Rinaudo, *Prog. Polym. Sci.*, **31**, 603 (2006), <https://doi.org/10.1016/j.progpolymsci.2006.06.001>
- ³⁴ K. Satoshi, M. Akira, K. Shigetaka and M. Yukiyoshi, *Int. J. Pharm.*, **56**, 125 (1989), [https://doi.org/10.1016/0378-5173\(89\)90005-7](https://doi.org/10.1016/0378-5173(89)90005-7)
- ³⁵ T. D. Pham, T. T. Bui, T. T. T. Truong, T. H. Hoang, T. S. Le *et al.*, *J. Mol. Liq.*, **298**, 111981 (2020), <https://doi.org/10.1016/j.molliq.2019.111981>
- ³⁶ M. H. Rasoulifard, S. Khanmohammadi and A. Heidari, *Water Sci. Technol.*, **74**, 1069 (2016), <https://doi.org/10.2166/wst.2016.230>
- ³⁷ A. Pandiarajan, R. Kamaraj and S. Vasudevan, *New J. Chem.*, **41**, 4518 (2017), <https://doi.org/10.1039/C6NJ04075F>
- ³⁸ W. S. Adriano, V. Veredas, C. C. Santana and L. B. Gonçalves, *Biochem. Eng. J.*, **27**, 132 (2005), <https://doi.org/10.1016/j.bej.2005.08.010>
- ³⁹ M. E. Mahmoud, A. M. El-Ghanam, R. H. A. Mohamed and S. R. Saad, *Mater. Sci. Eng. C*, **108**, 110199 (2020), <https://doi.org/10.1016/j.msec.2019.110199>
- ⁴⁰ Z. Li, X. Wang, X. Zhang, Y. Yang and J. Duan, *Chem. Eng. J.*, **413**, 127494 (2021), <https://doi.org/10.1016/j.cej.2020.127494>
- ⁴¹ T. K. Saha, R. K. Bishwas, S. Karmaker and Z. Islam, *ACS Omega*, **5**, 13358 (2020), <https://doi.org/10.1021/acsomega.0c01493>
- ⁴² P. Udaybhaskar, L. Iyengar and A. V. S. P. Rao, *J. Appl. Polym. Sci.*, **39**, 739 (1990), <https://doi.org/10.1002/app.1990.070390322>
- ⁴³ N. Sanli, S. Sanli, U. Sızır, M. Gumustas and S. A. Ozkan, *Chromatographia*, **73**, 1171 (2011), <https://doi.org/10.1007/s10337-011-2013-7>
- ⁴⁴ S. Karmaker, A. J. Nag and T. K. Saha, *Russ. J. Phys. Chem. A*, **94**, 2349 (2020), <https://doi.org/10.1134/S0036024420110126>
- ⁴⁵ T. K. Saha, N. C. Bhoumik, S. Karmaker, M. G. Ahmed, H. Ichikawa *et al.*, *Clean – Soil, Air, Water*, **39**, 984 (2011), <https://doi.org/10.1002/clen.201000315>
- ⁴⁶ M. Erşan, E. Bağda and E. Bağda, *Colloid. Surf. B: Biointerfaces*, **104**, 75 (2013), <https://doi.org/10.1016/j.colsurfb.2012.11.034>
- ⁴⁷ S. Y. Lagergren, *K. Sven. Vetenskapsakad. Handl.*, **24**, 1 (1898)
- ⁴⁸ Y. S. Ho and G. McKay, *Process Biochem.*, **34**, 451 (1999), [https://doi.org/10.1016/S0032-9592\(98\)00112-5](https://doi.org/10.1016/S0032-9592(98)00112-5)
- ⁴⁹ S. Y. Elovich and O. G. Larinov, *Izv. Akad. Nauk SSSR, Otd. Khim. Nauk.*, **2**, 209 (1962)
- ⁵⁰ Y. S. Ho and G. McKay, *Chem. Eng. J.*, **70**, 115 (1998), [https://doi.org/10.1016/S0923-0467\(98\)00076-1](https://doi.org/10.1016/S0923-0467(98)00076-1)
- ⁵¹ Z. Bekçi, Y. Seki and M. K. Yurdakoç, *J. Hazard. Mater.*, **133**, 233 (2006), <https://doi.org/10.1016/j.jhazmat.2005.10.029>
- ⁵² S. Karmaker, F. Sintaha and T. K. Saha, *Adv. Bio. Chem.*, **9**, 1 (2019), <https://doi.org/10.4236/abc.2019.91001>
- ⁵³ H. M. F. Freundlich, *Z. Phys. Chem.*, **57**, 385 (1906), <https://doi.org/10.1515/zpch-1907-5723>

⁵⁴ M. I. Temkin and V. Pyzhev, *Acta Physiochim. URSS*, **12**, 217 (1940)

⁵⁵ I. Langmuir, *J. Am. Chem. Soc.*, **40**, 1361 (1918), <https://doi.org/10.1021/ja02242a004>

⁵⁶ K. R. Hall, L. C. Eagleton, A. Acrivers and T. Vermenlem, *Ind. Eng. Chem. Fundam.*, **5**, 212 (1966), <https://doi.org/10.1021/i160018a011>

⁵⁷ L. S. Chan, W. H. Cheung, S. J. Allen and G. McKay, *Chin. J. Chem. Eng.*, **20**, 535 (2012), [https://doi.org/10.1016/S1004-9541\(11\)60216-4](https://doi.org/10.1016/S1004-9541(11)60216-4)

⁵⁸ J. G. Domszy and G. A. Roberts, *Macromol. Chem. Phys.*, **186**, 1671 (1985),

<https://doi.org/10.1002/macp.1985.021860815>

⁵⁹ G. L. Dotto and L. A. A. Pinto, *Carbohydr. Polym.*, **84**, 231 (2011),

<https://doi.org/10.1016/j.carbpol.2010.11.028>

⁶⁰ Y. Liu, *Colloid. Surf. A*, **274**, 34 (2006),

<https://doi.org/10.1016/j.colsurfa.2005.08.029>

⁶¹ A. Fakhri and S. Adami, *J. Taiwan Inst. Chem. Eng.*, **45**, 1001 (2014),

<https://doi.org/10.1016/j.jtice.2013.09.028>